Ultrafast Solvation Dynamics of Flavin Mononucleotide in the Reductase Component of p-Hydroxyphenylacetate Hydroxylase

ARTICLE *in* THE JOURNAL OF PHYSICAL CHEMISTRY B · JULY 2009

Impact Factor: 3.3 · DOI: 10.1021/jp901136y · Source: PubMed

Journal of Photochemistry and Photobiology A: Chemistry 234 (2012) 44–48

Contents lists available at SciVerse ScienceDirect

Journal of Photochemistry and Photobiology A: Chemistry

journal homepage: www.elsevier.com/locate/jphotochem

Conformational heterogeneity in pyranose 2-oxidase from *Trametes multicolor* revealed by ultrafast fluorescence dynamics

Haik Chosrowjan[a,*], Seiji Taniguchi[a], Thanyaporn Wongnate[b], Jeerus Sucharitakul[c], Pimchai Chaiyen[b], Fumio Tanaka[a,b,**]

[a] Division of Laser Biochemistry, Institute for Laser Technology, Utsubo-Honmachi, 1-8-4, Nishiku, Osaka 550-0004, Japan
[b] Department of Biochemistry, Center of Excellence in Protein Structure and Function, Faculty of Science, Mahidol University, Bangkok 10400, Thailand
[c] Department of Biochemistry, Faculty of Dentistry, Chulalongkorn University, Bangkok 10300, Thailand

ARTICLE INFO

Article history:
Available online 6 January 2012

Keywords:
Pyranose 2-oxidase
Flavoprotein
Conformational heterogeneity
ET reaction
Ultrafast fluorescence dynamic

ABSTRACT

Ultrafast fluorescence dynamics of flavin adenine dinucleotide (FAD) in wild type pyranose 2-oxidase (P2O) has been investigated in solution by means of fluorescence up-conversion method. Fluorescence decays were well described by two-exponential model function. Fluorescence lifetimes were $\tau_1 \sim 110$ fs and $\tau_2 \sim 360$ ps, respectively. The (τ_2/τ_1) ratio ($\sim$3200) was extraordinary high compared to other flavoproteins without subunit structure. The heterogeneous distribution of emission lifetimes were elucidated in terms of two different conformers of P2O; conformer 1 with τ_1 and conformer 2 with τ_2. Emission peaks of conformer 1 and conformer 2 were determined to be at $\sim$540 nm and 510 nm, respectively, using transient spectral reconstruction procedure. Using dynamics analysis by Kakitani and Mataga (KM) theory, both quenching processes were ascribed to photoinduced electron transfer (ET) reactions mainly from Trp168 to the excited isoalloxazine (Iso*) in different protein tetramers having different static dielectric constants ($\varepsilon_1 \sim 3.25$ for conformer 1 and $\varepsilon_2 \sim 5.93$ for conformer 2). The quaternary structure seems to be responsible for the observed conformational heterogeneity.

1. Introduction

Pyranose 2-oxidase is a flavin adenine dinucleotide (FAD)-dependent oxidase (P2O) present in the hyphal periplasmic space [1] of wood-degrading basidiomycetes [2,3]. P2O involves in lignin degradation by providing the essential co-substrate, H_2O_2, for manganese peroxidases [4–6]. P2O from *Trametes multicolor* is a homotetramer with a molecular mass of 270 kDa [7] where each of the four subunits carries one FAD molecule covalently bound to His167 via its 8α-methyl group [8]. Three dimensional structures of P2O from *Trametes multicolor* were determined by Hallberg et al. [9] and Kujawa et al. [10]. Reaction mechanisms of P2O have been studied by transient kinetics, kinetic isotope effects and site-directed mutagenesis [11–13]. The results show that P2O wild-type and the H167A mutant catalyze oxidation of D-glucose specifically at the glucose C2-position and the H-bonding at the flavin N5 is important for the flavin reduction and oxidation [13].

Fluorescence from isoalloxazine (Iso) is strongly quenched in many flavoproteins in which Trp and/or Tyr always exist near Iso. In such "non-fluorescent" flavoproteins it was demonstrated that the fluorescence exhibits ultrafast decays in the sub-picoseconds to several picoseconds time domain. This remarkable quenching phenomenon was elucidated in terms of photo-induced electron transfer (ET) from the Trp and/or Tyr to the excited Iso (Iso*) [13,14]. ET mechanisms in flavoproteins have been studied by ET theories and molecular dynamics simulations (MD) techniques [15,16]. For instance, the ET rate in flavin mononucleotide (FMN) binding protein could be reasonably well explained by taking the donor–acceptor distance, and the electrostatic (ES) energy between ionic groups and photoproducts in protein into consideration [17].

P2O contains Trp168 near Iso in every subunit, of which fluorescence is strongly quenched. According to the crystal structure of P2O [10], the donor–acceptor distances are almost identical in all four subunits. Therefore, P2O could be a good model for examining the effect of other factors, in addition to the donor–acceptor distance, on ET rate such as ES energy. In the present work, we have observed conformational heterogeneity in P2O enzyme by means of the fluorescence up-conversion technique, which could be explained in terms of heterogeneous dielectric constants of the Iso environment in the proteins.

2. Materials and methods

P2O was purified according to the method described elsewhere [10–12]. Ultrafast fluorescence dynamics were measured by a

* Corresponding author.
** Corresponding author. Present address: Department of Chemistry, Faculty of Science, Chulalongkorn University, Thailand.
E-mail address: haik@ilt.or.jp (H. Chosrowjan).

1010-6030/$ – see front matter © 2012 Elsevier B.V. All rights reserved.
doi:10.1016/j.jphotochem.2011.11.013

fluorescence up-conversion (~150 fs FWHM) method described in detail in earlier works [17,18]. Observed fluorescence decays could be well fitted using two-exponential model function (Eq. (1)).

$$F(\lambda, \quad t) = \alpha_1(\lambda)\exp\left\{\frac{-t}{\tau_1(\lambda)}\right\} + \alpha_2(\lambda)\exp\left\{\frac{-t}{\tau_2(\lambda)}\right\} \tag{1}$$

where $\tau_1(\lambda)$ and $\tau_2(\lambda)$ are emission wavelength-dependent time constants and $\alpha_1(\lambda)$ and $\alpha_2(\lambda)$ are corresponding fractions, respectively. The observed fluorescence dynamics of P2O was analyzed by Kakitani and Mataga (KM) ET theory [19] using P2O crystal structure data given in [10] (PDB code: 2IGK). The detailed method of the analysis was described in an earlier work [17] and is only briefly outlined below with an accent on main assumptions.

Based on our observations, we assumed that there are two P2O conformers with independent rate constants $k_{ET}^{ij}(m)$, where $m = 1$ and 2 are for conformers 1 and 2, respectively. We also assumed that all physical constants describing the static ET rate constants $k_{ET}^{ij}(m)$ [17] are independent of the conformer except for static dielectric constants ε_0^m. In $k_{ET}^{ij}(m)$, i denotes the ith subunit (A–D) in the protein tetramer and j denotes corresponding electron donating amino acids ($j = 1$ for Trp168, $j = 2$ for Trp253, $j = 3$ for Tyr456 and $j = 4$ for Tyr590). Donor–acceptor distances R_j^i between Iso and jth electron donor in ith subunit were expressed as center-to-center rather than edge-to-edge distances [15,19–22]. Protein systems contain many ionic groups, which may influence ET rate. Hence, ES (electrostatic) energy between Iso^- and all ionic groups including phosphate anions of FAD and between the donor j cation and all ionic groups in all four subunits have been included in the calculations. For reference, each subunit of P2O contains 31 Glu, 37 Asp, 26 Lys, 26 Arg amino acids and 2 negative charges at FAD phosphate. We assumed that all these groups are in an ionic state in solution. In the present work, ES energies were evaluated using only ionic groups in the protein. Addition of all partial charge densities in the protein for ES energy calculation did not change much the data obtained using the present simplified method. The calculated ET rate of conformer m, $k_{ET}^C(m)$, was determined by taking an average of all donors and all subunits (an average of $k_{ET}^{ij}(m)$ over i and j), and the corresponding lifetimes were determined as reciprocals of the ET rates. Finally, ET parameters were determined by minimizing χ^2 values in Eq. (2) by means of a non-linear least square method, according to Marquardt algorithm.

$$\chi^2 = \frac{\{1/\tau_1 - k_{ET}^C(1)\}^2}{k_{ET}^C(1)} + \frac{\{1/\tau_2 - k_{ET}^C(2)\}^2}{k_{ET}^C(2)} \tag{2}$$

for spectral identification of conformers 1 and 2, time-resolved fluorescence spectra with the fast and slow time constants were reconstructed from decay profiles using Eqs. (3) and (4), respectively.

$$F_1(\lambda, \quad t) = \alpha_1(\lambda)\frac{F_{SE}(\lambda)}{\alpha_1(\lambda)\tau_1(\lambda) + \alpha_2(\lambda)\tau_2(\lambda)}\exp\left\{\frac{-t}{\tau_1(\lambda)}\right\} \tag{3}$$

$$F_2(\lambda, \quad t) = \alpha_2(\lambda)\frac{F_{SE}(\lambda)}{\alpha_1(\lambda)\tau_1(\lambda) + \alpha_2(\lambda)\tau_2(\lambda)}\exp\left\{\frac{-t}{\tau_2(\lambda)}\right\} \tag{4}$$

Here $F_{SE}(\lambda)$ denotes fluorescence intensity at an emission wavelength λ under steady-state excitation condition.

3. Results

Fig. 1 shows the local structure near Iso (upper panel) and the quaternary structure (lower panel) of P2O. In this protein potential ET donors are Trp168, Trp253, Tyr456 and Tyr590 amino acids. Center to center (R_c), edge to edge (R_e) distances, and inter-planar angles between Iso and these aromatic amino acids are listed in Table S1 (Supplemental material). R_c between Iso and Trp168 was

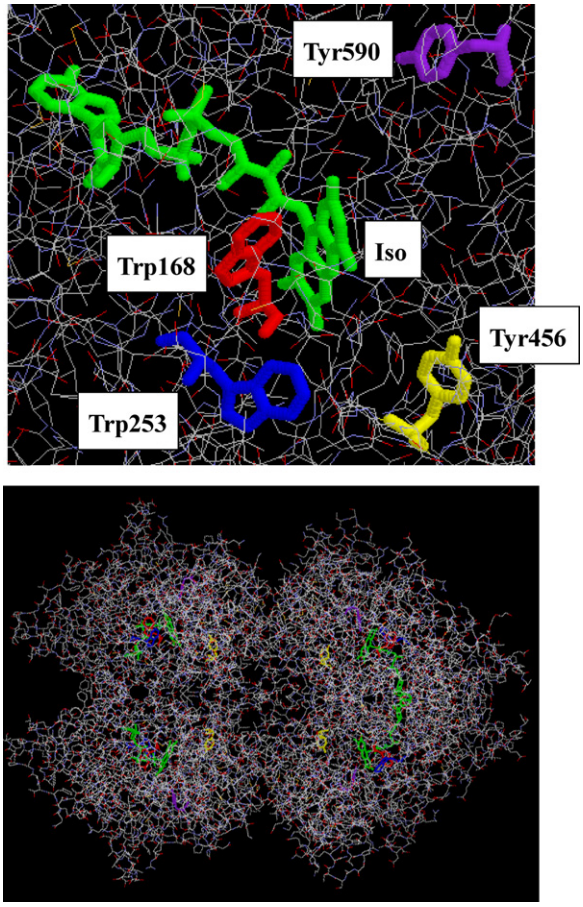

Fig. 1. Local structure near Iso and the quaternary structure of P2O. Iso, Trp168, Trp253, Tyr456 and Tyr590 are indicated in green, red, blue, yellow and purple, respectively. (For interpretation of the references to color in this figure legend, the reader is referred to the web version of the article.)

practically identical in all four subunits, ~0.61 nm. The R_c values between Iso and Trp253, Tyr456 and Tyr590 were ~1.1 nm, ~1.1 nm and ~1.3 nm, respectively, and only slightly varied among four subunits. The R_e values were around 0.35 nm, 0.81 nm, 0.67 nm and 0.84 nm for Trp168, Trp253, Tyr456 and Tyr590, respectively. These distances also did not differ much among different subunits.

Absorption and fluorescence spectra of P2O are shown in Fig. S1 (Supplemental material). The emission peak was at 510 nm, which is shorter compared to the fluorescence maximum of the free FAD (ca. 530 nm). Fig. 2 shows P2O fluorescence decays at different emission wavelengths in 10 ps time range. The values of shorter lifetimes $\tau_1(\lambda)$ were ~90 fs at 580 nm, ~110 fs at 555 nm and 530 nm, ~70 fs at 500 nm and ~57 fs at 480 nm, respectively. It is important to note that at shorter wavelengths the Raman line of water overlaps with the protein emission and may generate signals with very fast decays. By spectral reconstruction, we could clearly separate the Raman contribution at ca. 480 nm, as shown in Fig. 3. Hence, the rather faster decays at 480–500 nm spectral range may attribute to water Raman line contributions. The values of the longer lifetimes $\tau_2(\lambda)$ were ~360 ps at all monitored wavelengths. Accuracy of the longer lifetime value, however, may not be so high because it was beyond the dynamics range of present measurements. For more clarity, fluorescence decays in a longer and shorter dynamical ranges of 80 ps and 3 ps, respectively, are also shown in Fig. S2 (Supplemental material). It was noted that the ratio of $\tau_2(\lambda)/\tau_1(\lambda)$ was extraordinary high, ca. 3200, which has never been observed for other flavoproteins in earlier works [17,18,23]. We have carefully checked the reproducibility of these

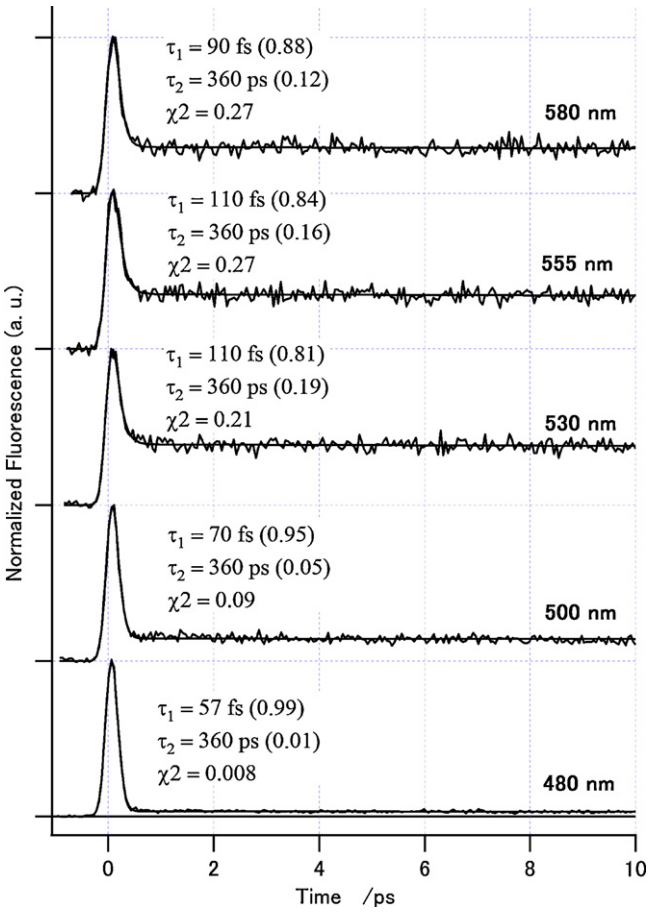

Fig. 2. Fluorescence decay dynamics of P2O protein at different emission wavelengths (excitation at 410 nm, ~17 mW). Double exponential fitting time constants, pre-exponential factors and χ^2 values are also indicated at each decay trace.

data and have confidence to exclude possible experimental artifacts such as impurities and gradual degradation (or denaturing) of protein samples. Hence, we interpret τ_1 and τ_2 as the lifetimes of FAD in two protein conformers: conformer 1 and conformer 2, respectively. Pre-exponential factors $\alpha_1(\lambda)$ and $\alpha_2(\lambda)$, given in inserts of Fig. 2, were emission-wavelength dependent. Time dependent fluorescence spectra (Fig. 3) of fast and slow conformers were obtained using Eqs. (3) and (4), respectively. The spectrum of slower conformer displays an emission peak at around 510 nm, is time-independent and similar to the fluorescence spectrum under steady-state excitation (see also Fig. S1 in Supplemental material). On the other hand, the spectrum of faster conformer seems as if it depends markedly upon the delay time. At $t = 0$ the intensity at 480 nm was highest and decreased quickly with the delay time. The emission peak at around 540 nm became visible at longer delay times. At ~1 ps of the delay time the intensity at 480 nm completely disappeared. These results and the spectral position of the water Raman line suggest that at the instant of excitation the Raman line of water which partially overlaps the conformer 1 spectrum, was dominant at ~480 nm but fast disappeared. As a result, it appeared that the spectrum of conformer 1 shifted by time toward the longer wavelengths and stabilized at 540 nm. In the reality, however, the conformer 1 spectrum is time independent with an emission peak centered at 540 nm.

As we have already mentioned, ET rates from all four donors to excited Iso* were determined by KM model theory [19] and the protein crystal structure [10] briefly described in Section 2 and in [17]. The physical quantities ν_0^q (adiabatic frequency), β^q (ET process coefficient), R_0^q (critical donor–acceptor distance) (q index denotes Trp or Tyr amino acids), static dielectric constants ε_0^1, ε_0^2 and standard Gibbs energy G_{Iso}^0 were determined according to a non-linear least square method. Among those ET parameters ν_0^q, β^q, R_0^q and G_{Iso}^0 were assumed to be common in both conformers, because the donor–acceptor distances were similar in all subunits. The values of these quantities were $\nu_0^{\mathrm{Trp}} = 1018\,\mathrm{ps}^{-1}$, $\nu_0^{\mathrm{Tyr}} = 197\,\mathrm{ps}^{-1}$, $\beta^{\mathrm{Trp}} = 21.0\,\mathrm{nm}^{-1}$, $\beta^{\mathrm{Tyr}} = 6.26\,\mathrm{nm}^{-1}$, $R_0^{\mathrm{Trp}} = 0.874\,\mathrm{nm}$, $R_0^{\mathrm{Tyr}} = 0.499\,\mathrm{nm}$ and $G_{\mathrm{Iso}}^0 = 7.28\,\mathrm{eV}$. The dielectric constants of conformer 1 and conformer 2 were determined to be $\varepsilon_0^1 \sim 3.25$ and $\varepsilon_0^2 \sim 5.93$, respectively. The calculated ET rates of conformers 1 and 2, which were obtained as sums of all $k_{\mathrm{ET}}^{ij}(m)$, were 11.3 (ps^{-1}) and 2.79×10^{-3} (ps^{-1}), respectively. The corresponding lifetimes are 88.4 fs and 358 ps, respectively, which are quite close to the observed ones (~110 fs and ~360 ps).

Table 1 lists solvent reorganization energies $-\lambda_S^{ij}(m)$, net ES energies $\mathrm{ES}_i^j(m)$, ES energies between donor cations and Iso anions $-e^2/\varepsilon_0^m R_j^i$ and ET rates $k_{\mathrm{ET}}^{ij}(m)$ from various donors. The calculations show that the ET takes place mostly from Trp168 in all subunits and rates from the donors other than Trp168 were all negligibly slow (Table 1). Variations in $\lambda_S^{ij}(m)$, $-e^2/\varepsilon_0^m R_j^i$ and $\mathrm{ES}_i^j(m)$ were comparably small among the subunits for a given conformer. $k_{\mathrm{ET}}^{ij}(m)$ slightly varied from 12.3 (ps^{-1}) in the subunit B to 10.8 (ps^{-1}) in the subunit A (conformer 1) and from 3.07×10^{-3} (ps^{-1}) in the subunit D to 2.63×10^{-3} (ps^{-1}) in the subunit A (conformer 2). The mentioned parameters, however, greatly vary between conformers 1 and 2, and were ascribed to the difference in the calculated static dielectric constants, $\varepsilon_0^1 = 3.25$ and $\varepsilon_0^2 = 5.93$ corresponding to conformers 1 and 2, respectively.

4. Discussion

The physical basis for the obtained difference in the dielectric constants of conformers 1 and 2 is not clear at present. For conventional cases, according to Onsager model, a dielectric constant in pure liquids depends on a dipole moment of solvent molecules [26]. Kirkwood and Froehlich introduced the so called "Kirkwood correlation factor" into Onsager equation, which depends on specific molecular interactions between molecules [26]. In case of the proteins, the picture is much more complicated. There are many ionic amino acids and the sum of their dipole moments over all constituents may be much greater than those of organic solvents. Another characteristic of the proteins vs. pure liquids is heterogeneous distribution of various amino acids, whereas the molecular distribution is uniform in pure liquid. For a P2O case, the heterogeneity of a substrate loop from residues 452–457 were observed in P2O crystal structures. This loop is located near Iso [10,24,25]. The data indicate that the structure around Iso is flexible and may be the cause of the conformational heterogeneity observed by the fluorescence data reported herein. Therefore, ultrafast fluorescence spectroscopy can be a useful tool for probing dynamics of the loop movement in future investigations. On the other hand, it is also possible that the heterogeneity in fluorescence lifetimes is due to the heterogeneity in subunits of the tetramer in solution, because no monomeric flavoprotein has displayed such a great difference in the characteristic lifetimes [17,18,23]. In our present analysis, all distances between donor and acceptor were fixed and significant heterogeneity of amino acids near flavin was considered causing the big energy gap difference. In such case, other factors like driving force, vibrational reorganization energy, and electronic coupling, may also change and affect the reaction. How much is the heterogeneity near flavin contributes to observed time constant difference and how much is the contribution of possible distance

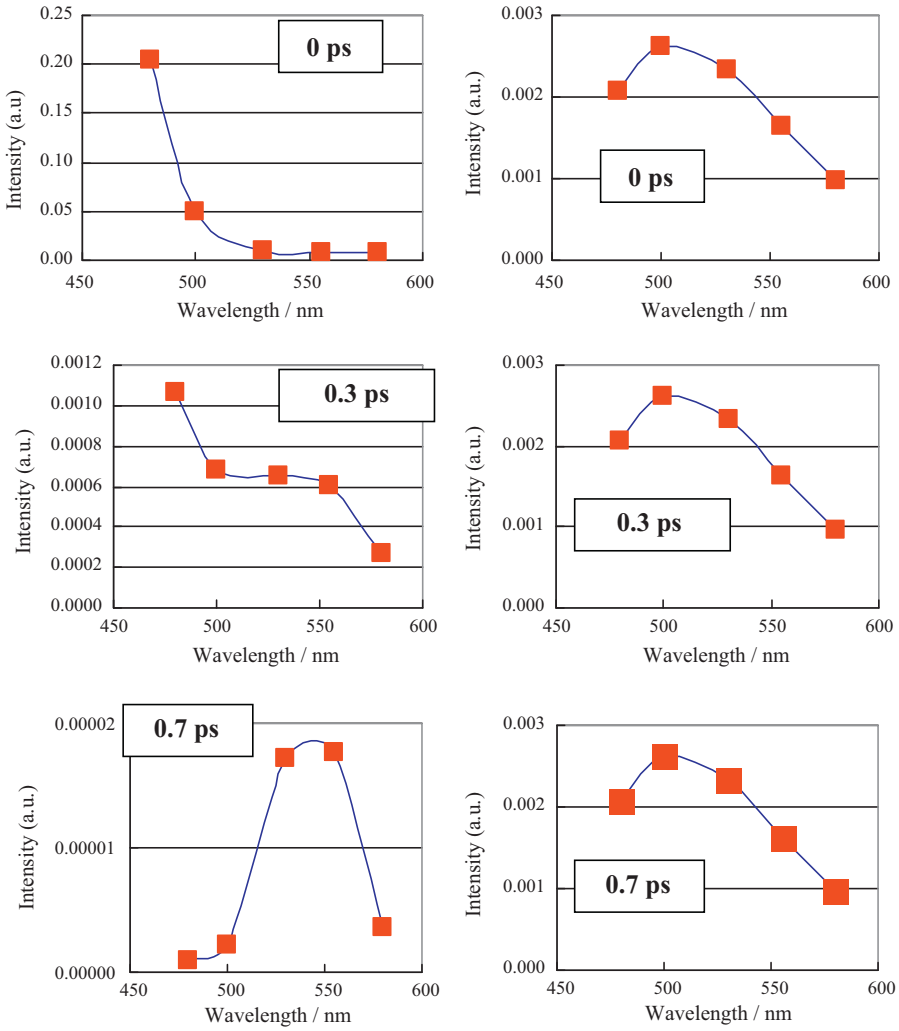

Fig. 3. Reconstructed time-resolved fluorescence spectra of P2O. Inserts indicate delay times after excitation. Spectra at left correspond to the conformer 1 with the decay time $\tau_1(\lambda)$ and at right to the conformer 2 with the decay time $\tau_2(\lambda)$, respectively. The spike at 480 nm is due to the Raman scattering of water.

Table 1
Physical quantities related to the ET process; solvent reorganization energies $\lambda_S^{ij}(m)$, net ES energies $ES_i^j(m)$, ES energies between donor cations and Iso anions $-e^2/\varepsilon_0^m R_j^i$ and ET rates $k_{ET}^{ij}(m)$ from all four donors in each subunit.

Physical quantities	Subunits	Trp168		Trp253		Tyr456		Tyr590	
		Conf 1	Conf 2	Conf 1	Conf 2	Conf 1	Conf 2	Conf 1	Conf 2
$\lambda_S^{ij}(m)$ (eV)	A	0.899	1.55	1.09	1.88	1.27	2.19	1.19	2.06
	B	0.898	1.55	1.09	1.89	1.27	2.19	1.19	2.06
	C	0.898	1.55	1.09	1.88	1.27	2.19	1.19	2.06
	D	0.896	1.55	1.09	1.88	1.27	2.19	1.19	2.06
$ES_i^j(m)$ (eV)	A	0.223	0.122	1.22	0.669	0.719	0.394	−0.152	−0.083
	B	0.211	0.115	1.17	0.643	0.722	0.396	−0.155	−0.085
	C	0.222	0.122	1.17	0.639	0.701	0.384	−0.156	−0.086
	D	0.215	0.118	1.19	0.650	0.670	0.367	−0.174	−0.096
$-e^2/\varepsilon_0^m R_j^i$ (eV)	A	−0.679	−0.372	−0.369	−0.202	−0.233	−0.127	−0.359	−0.197
	B	−0.681	−0.373	−0.368	−0.201	−0.233	−0.128	−0.357	−0.195
	C	−0.680	−0.373	−0.368	−0.202	−0.234	−0.128	−0.358	−0.196
	D	−0.683	−0.374	−0.369	−0.202	−0.232	−0.127	−0.357	−0.196
$k_{ET}^{ij}(m)$ (ps^{-1})	A	10.8	0.00263	9.84×10^{-16}	6.36×10^{-14}	1.15×10^{-32}	8.03×10^{-32}	6.81×10^{-13}	6.30×10^{-19}
	B	12.3	0.00305	4.07×10^{-15}	1.01×10^{-13}	1.12×10^{-32}	8.30×10^{-32}	5.60×10^{-13}	5.14×10^{-19}
	C	11.1	0.00273	5.57×10^{-15}	1.20×10^{-13}	2.96×10^{-32}	1.35×10^{-31}	6.46×10^{-13}	5.80×10^{-19}
	D	12.2	0.00307	3.08×10^{-15}	9.78×10^{-14}	7.48×10^{-32}	1.72×10^{-31}	9.19×10^{-13}	6.92×10^{-19}

changes between donor and acceptor in different conformers? The present work did not address these possibilities, but future investigations on P2O mutant protein (T169A, H167A, H167A/H548A, H167A/H548N) dynamics will shed more light on the P2O dynamics in solution, especially how the changes in the geometrical factors between ET donor and acceptor are related to the change in the ET rate.

Acknowledgments

This work was partially supported by grants from the Thailand Research Fund No. BRG5480001 and from Faculty of Science, Mahidol University (to P.C.)

Appendix A. Supplementary data

Supplementary data associated with this article can be found, in the online version, at doi:10.1016/j.jphotochem.2011.11.013.

References

[1] G. Daniel, J. Volc, E. Kubátová, Appl. Environ. Microbiol. 60 (1994) 2524.
[2] J. Volc, N.P. Denisova, F. Nerud, V. Musıĭlek, Folia Microbiol. 30 (1985) 141.
[3] C. Leitner, D. Haltrich, B. Nidetzky, H. Prillinger, K.D. Kulbe, Appl. Biochem. Biotechnol. 70–72 (1998) 237.
[4] R. ten Have, P. Teunissen, J. Chem. Rev. 101 (2001) 3397.
[5] P. Ander, L. Marzullo, J. Biotechnol. 53 (1997) 115.
[6] J. Volc, E. Kubátová, G. Daniel, V. Prikrylová, Arch. Microbiol. 165 (1996) 421.
[7] C. Leitner, J. Volc, D. Haltrich, Appl. Environ. Microbiol. 67 (2001) 3636.
[8] P. Halada, C. Leitner, P. Sedmera, D. Haltrich, J. Volc, Anal. Biochem. 314 (2003) 235.
[9] B.M. Hallberg, C. Leitner, D. Haltrich, C. Divne, J. Mol. Biol. 341 (2004) 781.
[10] M. Kujawa, H. Ebner, C. Leitner, B.M. Hallberg, M. Pronjit, J. Sucharitakul, R. Ludwig, U. Rudsander, C. Peterbauer, P. Chaiyen, D. Haltrich, C. Divne, J. Biol. Chem. 281 (2006) 35104.
[11] M. Prongjit, J. Sucharitakul, T. Wongnate, D. Haltrich, P. Chaiyen, Biochemistry 48 (2009) 4170.
[12] J. Sucharitakul, T. Wongnate, P. Chaiyen, Biochemistry 49 (2010) 3753.
[13] (a) A. Karen, M.T. Sawada, F. Tanaka, N. Mataga, Photochem. Photobiol. 45 (1987) 49;
(b) W. Pitsawong, J. Sucharitakul, M. Prongjit, T.C. Tan, O. Spadiut, D. Haltrich, C. Divne, P. Chaiyen, J. Biol. Chem. 285 (2010) 9697.
[14] (a) C. Aubert, P. Mathis, A.P.M. Eker, K. Brettel, Proc. Natl. Acad. Sci. U.S.A. 96 (1999) 5423;
(b) M. Byrdin, A.P.M. Eker, M.H. Vos, K. Brettel, Proc. Natl. Acad. Sci. U.S.A. 100 (2003) 8676;
(c) D.P. Zhong, A.H. Zewail, Proc. Natl. Acad. Sci. U.S.A. 98 (2001) 11867;
(d) G. Kodali, S.U. Siddiqui, R.J. Stanley, J. Am. Chem. Soc. 131 (2009) 4795.
[15] N. Nunthaboot, F. Tanaka, S. Kokpol, H. Chosrowjan, S. Taniguchi, N. Mataga, J. Phys. Chem. B 112 (2008) 13121.
[16] N. Nunthaboot, F. Tanaka, S. Kokpol, H. Chosrowjan, S. Taniguchi, N. Mataga, J. Photochem. Photobiol. A: Chem. 209 (2010) 79.
[17] H. Chosrowjan, S. Taniguchi, N. Mataga, T. Nakanishi, Y. Haruyama, S. Sato, M. Kitamura, F. Tanaka, J. Phys. Chem. B 114 (2010) 6175.
[18] H. Chosrowjan, S. Taniguchi, N. Mataga, F. Tanaka, D. Todoroki, M. Kitamura, Chem. Phys. Lett. 462 (2008) 121.
[19] (a) T. Kakitani, N. Yoshimori, N. Mataga, in: J.R. Bolton, N. Mataga, G. McLendon (Eds.), Advances in Chemistry Series, 228, American Chemical Society, Washington, DC, 1991, pp. 45–69;
(b) T. Kakitani, A. Yoshimori, N. Mataga, J. Phys. Chem. 96 (1992) 5385–5392;
(c) T. Kakitani, N. Matsuda, A. Yoshimori, N. Mataga, Prog. React. Kinet. 20 (1995) 347–375.
[20] N. Nunthaboot, F. Tanaka, S. Kokpol, H. Chosrowjan, S. Taniguchi, N. Mataga, J. Photochem. Photobiol. A 201 (2009) 191.
[21] (a) R.A. Marcus, J. Chem. Phys. 24 (1956) 966–978;
(b) R.A. Marcus, Annu. Rev. Phys. Chem. 15 (1964) 155–196;
(c) C. Moser, J. Keske, K. Warncke, R. Farid, P. Dutton, Nature 355 (1992) 796.
[22] V. Vorsa, T. Kono, K.F. Willey, L. Winograd, J. Phys. Chem. B 103 (1999) 7889.
[23] H. Chosrowjan, S. Taniguchi, N. Mataga, F. Tanaka, D. Todoroki, M. Kitamura, J. Phys. Chem. B 111 (2007) 8695.
[24] T.C. Tan, W. Pitsawong, T. Wongnate, O. Spadiut, D. Haltrich, P. Chaiyen, C. Divne, J. Mol. Biol. 402 (2010) 578.
[25] O. Spadiut, T.C. Tan, I. Pisanelli, D. Haltrich, C. Divne, FEBS J. 277 (2010) 2892.
[26] C.J.F. Boettcher, Theory of Electric Polarization, 2nd ed., Elsevier, Amsterdam, 1973.